Original Article

Transcriptomic Landscape Analysis Reveals a Persistent DNA Damage Response in Metabolic Dysfunction-associated Steatohepatitis Post-dietary Intervention

Zi-Yuan Zou[1,2#], Tian-Yi Ren[1#], Jia-Qi Li[2,3], Ting-Ying Jiao[2,4], Meng-Yu Wang[1], Lei-Jie Huang[5], Shuang-Zhe Lin[1], Yuan-Yang Wang[2], Xiao-Zhen Guo[2], Ye-Yu Song[1,2], Rui-Xu Yang[1], Cen Xie[2,3*] and Jian-Gao Fan[1,6*]

[1]Center for Fatty Liver, Department of Gastroenterology, Xinhua Hospital Affiliated to Shanghai Jiao Tong University School of Medicine, Shanghai, China; [2]State Key Laboratory of Drug Research, Shanghai Institute of Materia Medica, Chinese Academy of Sciences, Shanghai, China; [3]University of Chinese Academy of Sciences, Beijing, China; [4]Human Phenome Institute, School of Life Sciences, Fudan University, Shanghai, China; [5]Department of Gastroenterology, Ningbo No. 2 Hospital, Ningbo, Zhejiang, China; [6]Shanghai Key Laboratory of Pediatric Gastroenterology and Nutrition, Shanghai, China

Abstract

Background and Aims: Metabolic dysfunction-associated steatotic liver disease (MASLD) and its more advanced form, metabolic dysfunction-associated steatohepatitis, have emerged as the most prevalent liver diseases worldwide. Currently, lifestyle modification is the foremost guideline-recommended management strategy for MASLD. However, it remains unclear which detrimental signals persist in MASLD even after disease remission. Thus, we aimed to examine the persistent changes in liver transcriptomic profiles following this reversal. ***Methods:*** Male C57BL/6J mice were divided into three groups: Western diet (WD) feeding, chow diet (CD) feeding, or diet reversal from WD to CD. After 16 weeks of feeding, RNA sequencing was performed on the mice's livers to identify persistent alterations characteristic of MASLD. Additionally, RNA sequencing databases containing high-fat diet-fed P53-knockout mice and human MASLD samples were utilized. ***Results:*** WD-induced MASLD triggered persistent activation of the DNA damage response (DDR) and its primary transcription factor, P53, long after the resolution of the hepatic phenotype through dietary reversal. Elevated levels of P53 might promote apoptosis, thereby exacerbating metabolic dysfunction-associated steatohepatitis, as they strongly correlated with hepatocyte ballooning, an indicator of apoptosis activation. Moreover, P53 knockout in mice led to downregulated expression of apoptosis signaling in the liver. Mechanistically, P53 may regulate apoptosis by transcriptionally activating the expression of apoptosis-enhancing nuclease (AEN). Consistently, P53, AEN, and the apoptosis process

all exhibited persistently elevated expression and showed a strong inter-correlation in the liver following dietary reversal. ***Conclusions:*** The liver demonstrated upregulation of DDR signaling and the P53-AEN-apoptosis axis both during and after exposure to WD. Our findings provide new insights into the mechanisms of MASLD relapse, highlighting DDR signaling as a promising target to prevent MASLD recurrence.

Introduction

With the continuous consumption of Western-style diets and the obesity pandemic, nonalcoholic fatty liver disease (NAFLD), now rebranded as metabolic dysfunction-associated steatotic liver disease (MASLD), has become the predominant cause of chronic liver disease worldwide, with an approximate prevalence of 38.0%.[1–3] Up to one-third of individuals with MASLD are classified into metabolic dysfunction-associated steatohepatitis (MASH) with or without fibrosis, which can ultimately lead to liver cirrhosis, liver failure, and cancer.[4–6] It was not until this year that resmetirom was approved by the United States Food and Drug Administration for the treatment of MASH. However, its use is indicated only in MASH patients with F2 and F3 stage fibrosis that have not yet progressed to cirrhosis, indicating that there remains a substantial and unmet clinical need. The most effective and safe intervention remains weight loss, which can be achieved through lifestyle modifications, particularly dietary shifting from an unhealthy to a healthy regimen.[7,8]

The effectiveness and long-term adherence of dietary interventions in MASLD patients have been established over the past two decades. Specifically, the Mediterranean diet, known for its low-fat and low-cholesterol characteristics, has

shown promise in reducing the incidence of MASLD, as demonstrated in a cohort study involving 1,521 participants.[9] Consequently, both European and Asian guidelines recommend adopting a Mediterranean dietary pattern for managing macronutrient intake in MASLD patients.[10,11] Moreover, the effectiveness of dietary interventions for MASLD has been supported by research in mice. Transitioning mice from a high-fat and high-fructose diet to a chow diet (CD) was found to reverse key histological changes of MASLD, including steatosis, liver inflammation, and fibrosis in an experimental MASH model.[12] Despite these advancements, uncertainties still exist regarding dietary interventions for MASLD, particularly concerning the long-term liver-related outcomes of individuals who achieved MASLD remission through dietary changes, as well as in healthy individuals who have never experienced MASLD.

The limited understanding of MASH following dietary intervention makes it challenging to predict the likelihood of recurrence in MASH, especially since the recurrence rates of MASLD are as high as 49.0%, surpassing its prevalence.[13] This high recurrence rate, coupled with its prevalence, imposes substantial economic and clinical burdens.[14,15] However, little research addresses the risk factors and mechanisms of MASLD recurrence. Current knowledge largely relies on existing research on the recurrence of obesity, which is the primary cause of MASLD.[16] A recent study discovered the long-term effects of obesity history on the immune response in later life,[17] prompting further inquiry into its lasting influence on hepatic metabolism and inflammation. Notably, a history of obesity is directly associated with the risk of hepatocellular carcinoma and serves as an independent predictor of this cancer in patients with cirrhosis.[18] Given the high recurrence rate of MASLD, we propose that although dietary intervention can reverse the histological features of MASLD, previous exposure to a Western diet (WD) and a history of MASLD might induce persistent alterations in liver transcriptomic profiles that have yet to be fully understood.

The present study aimed to evaluate the therapeutic effects of transitioning from a WD back to a CD and examine the persistent changes in liver transcriptomic profiles following this reversal. Using a MASH mouse model induced by a WD, we observed that switching from WD to CD (WD→CD) significantly improved steatosis, ballooning, and lobular inflammation in the liver. Analysis of RNA-seq data revealed that the DNA damage response (DDR) pathway, which was initially activated in MASLD, remained activated even after the diet reversal. P53 was further identified as a key regulator of DDR signaling in MASLD, and it upregulated the expression of apoptosis-enhancing nuclease (AEN) in the liver. AEN has been identified as a direct transcriptional target of P53 and established as necessary for inducing apoptosis in cancer cell lines.[19,20] Overall, these findings suggest that DDR signaling and the P53-AEN axis remain activated in the liver following the transition from a WD to a CD, even when MASLD is histologically resolved. This highlights the potential contribution of the DDR pathway to MASLD recurrence.

Methods

Animal studies

Specific pathogen-free male C57BL/6J mice, eight weeks of age, and 20 to 22 g body weight (Shanghai Laboratory Animal Center, Shanghai, China), were maintained under a standard 12 h dark/light cycle with water and diet provided ad libitum. After seven days of acclimatization, the mice were randomly divided into three groups for a 16-week dietary intervention: (i) CD (TrophicDiet, Nantong, China) as detailed previously; (ii) WD (TrophicDiet, Nantong, China) including 88% CD, 10% lard, and 2% cholesterol by weight[21,22]; (iii) dietary reversal (WD→CD), where mice were given WD for eight weeks followed by eight additional weeks of CD. The energy sources of both diets are shown in Supplementary Table 1. All animal experiments were approved by the Institutional Animal Care and Use Committee of Xinhua Hospital affiliated to Shanghai Jiao Tong University School of Medicine and were conducted in accordance with the guidelines of the National Research Council Guide for Care and Use of Laboratory Animals. At the end of 16 weeks, the mice were anesthetized with isoflurane and subsequently sacrificed for tissue sampling.

Biochemical analysis

For serum indices, levels of ALT and AST were measured following the instructions provided with each assay kit (Jiancheng, Nanjing, China). To analyze liver triglycerides and cholesterol, frozen liver samples (20 mg) were homogenized using a hybrid grinding machine (Biheng Bio-Technique Co. Ltd., Shanghai, China) in a 10% (weight/volume) 50 mmol/L Tris solution containing 1% Triton X-100. After centrifugation at 3,500 rpm, the resulting supernatants were quantified using each assay kit (Jiancheng, Nanjing, China).

Histologic assessment

Liver tissue samples were fixed in a 10% formalin solution for 24–48 h, dehydrated, and paraffin-embedded. The sections were stained with hematoxylin and eosin. Brightfield images were scanned with the NanoZoomer 2.0-HT slide scanner (Hamamatsu, Japan) at different magnifications. The NAFLD activity score was evaluated blindly as previously described.[23,24]

Huh7 cell culture and treatment

Human hepatocarcinoma cells (Huh7 cell line) were purchased from ATCC and cultured in DMEM medium supplemented with 10% fetal bovine serum and 1% penicillin-streptomycin (all from Gibco) at 5% CO_2 and 37°C. Palmitic acid (PA) was purchased from Sigma-Aldrich.

Three rounds of PA stimulation experiments were conducted. In Experiment 1, cells were assigned to one of two conditions: one set was introduced to fresh media with 0.4 mM PA for a 24-h period, while the controls were incubated in PA-free medium for the same duration.

For the second experiment, a two-phase intervention was implemented with three groups. One group was exposed to 0.4 mM PA for 24 h, followed by a 24-h period in PA-free medium. Cells kept in a PA-free medium for the full 48-h duration served as the negative control group. The positive control group had cells initially in a PA-free medium followed by a 24-h period in 0.4 mM PA.

Experiment 3 contained three interventions with cells distributed into three groups: (i) maintained in PA-free medium for 72 h, (ii) initially treated with 0.4 mM PA for 24 h, thereafter transferred to PA-free medium for another 24 h, and lastly reintroduced to 0.4 mM PA for an additional 24 h, and (iii) cells initially sustained in PA-free medium for 48 h followed by 24 h in 0.4 mM PA.

Cytotoxicity assessment of Huh7

Huh7 cells were seeded at 1.5×10^4 cells/well in 96-well plates, and the procedures for the experiments followed

those delineated in PA stimulation experiments 1, 2, and 3. Finally, cells were introduced to fresh media with 10% CCK-8 (Meilun Bio, Dalian, China) at 37°C for 1 h. The absorbance was measured at 450 nm.

Western blot analysis

Livers were lysed with an SDS sample buffer containing a protease inhibitor cocktail (Meilun Bio, Dalian, China) and phenylmethylsulfonyl fluoride (Meilun Bio, Dalian, China). Protein concentration was determined using the BCA Protein Assay Kit (Meilun Bio, Dalian, China). The proteins were separated by sodium dodecyl sulfate-polyacrylamide gel electrophoresis and transferred onto a polyvinylidene difluoride membrane. The membranes were blocked with Protein-Free Quick Blocking buffer (Meilun Bio, Dalian, China) and incubated with primary antibodies against α-tubulin (sc-5286, Santa Cruz), Vinculin (66305-1-Ig, Proteintech), P53 (2524, Cell Signal Technology), and phospho-histone H2A.X Ser 139 (sc-517348, Santa Cruz). After washing, anti-mouse IgG was used as the secondary antibody. The blots were rewashed and developed by chemiluminescence (Immobilon Western Chemiluminescent Horseradish Peroxidase substrate, Meilun Bio, Dalian, China).

Mouse RNA-seq library preparation and sequencing

RNA was extracted from frozen mouse liver tissue using Trizol reagent (Life Technologies, California, USA). The quality of RNA was assessed with the kaiaoK5500® Spectrophotometer (Kaiao, Beijing, China). Library construction and sequencing were conducted by Biomarker Technologies. The Illumina TruSeq RNA Sample kit (Illumina, San Diego, CA) was used to create strand-specific libraries following the manufacturer's instructions. Library products were purified with the AMPure XP system (Beckman Coulter, Beverly, USA) and validated by the Agilent 2100 bioanalyzer (Agilent Technologies, USA). The samples were sequenced on the Illumina NovaSeq 6000 (Illumina, USA). The clean reads were then mapped to the mouse reference genome sequence, and the uniquely mapped fragments of each gene were counted by StringTie (version 1.3.0).[25] Expression levels of different samples were calculated as Fragments Per Kilobase of transcript per Million mapped fragments (hereinafter referred to as FPKM).[26] The FPKM values were normalized using the scale method with the "limma" R package and log2-transformed (after adding 1 to avoid undefined values).

Differential expression analysis

The "limma" R package was utilized to screen for differentially expressed genes (DEGs) between the CD, WD, and WD→CD groups.[27] An unadjusted *p*-value < 0.05 and |log2 fold-change| > 0.5 were used as the cutoff values to determine DEGs, indicating statistical significance. Genes that were upregulated in both the WD and WD→CD groups, compared to the CD group, were defined as consistently upregulated genes. Genes that were downregulated in both the WD and WD→CD groups, compared to the chow group, were defined as consistently downregulated genes. Consistently regulated genes were defined as the sum of consistently upregulated and downregulated genes. Additionally, P53 target genes were selected according to previous studies.[28–30]

Gene function annotations

Gene Ontology biological processes and molecular function term enrichment analysis were conducted on the specific gene sets using the "ClusterProfiler" R package.[31] A *p*-value < 0.05 was deemed statistically significant.

Gene set enrichment analysis

Following differential expression analysis, we employed the "clusterProfiler" R package to conduct gene set enrichment analysis (GSEA),[31,32] with reference to the Wikipathways and Gene Ontology database.[33,34] Moreover, a normalized enrichment score was used to quantify the enrichment level of the specific pathways. A *p*-value < 0.05 was deemed statistically significant. Additionally, the GSEA results were visualized using the "enrichplot" R package.[31]

Single-sample gene set enrichment analysis (ssGSEA)

The pathways were deconvoluted in the RNA sequencing data using the ssGSEA method. The gene sets of pathways were downloaded from the Molecular Signature Database (MsigDB v7.1, www.broadinstitute.org/msigdb). The ssGSEA scores were quantified using the "GSVA" R package. Additionally, we estimated the relative expression of liver non-parenchymal cells based on single-cell RNA-seq data from five healthy and five cirrhotic livers.[35] Cell types with a median expression equal to or below 0 were removed. Lastly, we performed programmed cell death (PCD) subset deconvolution. The gene lists of six PCD types, including autophagy, entotic cell death, ferroptosis, lysosome-dependent cell death, necroptosis, and pyroptosis, were extracted from a previous report.[36] The genes related to liver non-parenchymal cells and PCD, used for deconvolution analysis, were listed in Supplementary Tables 2–5.

Calculation of NAFLD relevance score

We searched the GeneCards database (https://www.genecards.org/) to identify genes associated with NAFLD.[37] Using the keyword "nonalcoholic fatty liver disease", we obtained relevance scores for each gene, enabling us to sort them into specific gene sets based on their NAFLD relevance scores.

Open-access data collection and normalization

The Gene Expression Omnibus (GEO) database (http://www.ncbi.nlm.nih.gov/geo/) was systematically searched. Ultimately, two large human datasets (GEO dataset ID: GSE135251 and GSE89632) were selected for this study. Additionally, we included a database (GEO dataset ID: GSE176112) of RNA sequencing data from mouse livers. This database includes three high-fat diet (HFD)-fed P53-knockout mice and three HFD-fed wild-type mice. Supplementary Table 6 provides a summary of the basic information of these datasets extracted from the GEO database. All gene expression profiling data were normalized using the scale method with the "limma" R package.[27]

Data visualization

We performed Principal Component Analysis (PCA) to examine the distribution differences of each group using the "ggbiplot" R package.[38] Heatmaps of DEGs were generated using the "pheatmap" R package.[39] We created correlation heatmaps using the Lianchuan Biological website (https://www.omicstudio.cn/tool).[40] The Venn diagrams were generated using EVenn (http://www.ehbio.com/test/venn/).[41] DotChart plots were created using Hiplot Pro (https://hiplot.com.cn/).[42] Bubble plots were generated using the "ggplot2" R package.[31] Finally, we conducted linear regression and visualized the data using the "ggpubr" R package.[43]

Statistical analysis

Experimental data are presented as the mean ± SEM. Com-

parisons between groups were performed using the Student's *t*-test for two groups or one-way ANOVA for more than two groups. Additionally, Pearson correlation or Spearman correlation tests were applied to determine correlations. *p*-values less than 0.05 were considered statistically significant. All statistical analyses were carried out using GraphPad Prism 8.0 software (San Diego, CA) and R software (version 3.6.3).

Results

Diet intervention reverses the MASLD-related phenotype in mice

To assess the long-term negative effects of a WD on liver function post-exposure, we utilized the WD-induced MASLD mouse model.[21,22] Mice were subjected to either a CD or WD for 16 weeks, with the dietary reversal group receiving eight weeks of WD followed by eight weeks of CD (WD→CD, Fig. 1A). Compared to CD-fed mice, WD-fed mice displayed pronounced lipid accumulation and hepatocyte ballooning degeneration in the liver. However, the WD→CD group showed a significant reversal of hepatic steatosis (Fig. 1B). Regarding the NAFLD activity score, WD-fed mice exhibited elevated scores for steatosis, lobular inflammation, and ballooning compared to the CD group. Conversely, the WD→CD mice showed similar scores to CD-fed mice for these indices (Fig. 1C-F). Biochemical tests on liver and serum indicated heightened levels of serum ALT and AST, as well as liver triglycerides and cholesterol, in the 16-week WD group compared to the CD group. The WD→CD group, however, showed complete restoration to normal levels of these biochemical parameters (Fig. 1G-J). These findings underscore that the dietary switch successfully ameliorated liver injury and aberrant lipid metabolism in mice fed a WD.

Furthermore, RNA-seq analysis was employed to gain further insights into liver inflammation and fibrosis across the groups. PCA showed significant separation among the three groups, indicating distinct transcriptomic patterns (Fig. 2A). ssGSEA analysis corroborated inflammation and fibrosis levels across the groups. Pathways related to cytokine production during the inflammatory response and collagen biosynthesis exhibited similar deconvolution scores in both the CD and WD→CD groups, significantly lower than those in the 16-week WD group (Fig. 2B). Collectively, these pathway analyses suggest that the dietary transition effectively mitigated hepatic inflammation and fibrosis induced by WD. Abnormal cytokine production is a key pathogenic event in lobular inflammation associated with MASLD. Consistently, GSEA revealed that the pathways related to cytokine production were significantly activated in the 16-week WD group compared to the CD group. However, these pathways were markedly suppressed following the eight-week dietary reversal (Fig. 2C-D). In concordance with the cytokine pathway results, further exploration into the impact of dietary transition on the liver microenvironment through cell-type decomposition analysis unveiled significant normalization of non-parenchymal cell types upregulated by WD feeding, such as endothelial cells, mesenchymal cells, mast cells, mononuclear phagocytes, B cells, plasmacytoid dendritic cells, and T cells (Fig. 2E-G). These non-parenchymal cells have been implicated in the pathogenesis of MASLD-associated inflammation and fibrosis. Overall, these results suggest that the inflammatory response was substantially restored by an eight-week dietary intervention. Furthermore, it is critical to note that numerous programmed cell death pathways seem to reverse following dietary reversal. Our deconvolution analysis identified six specific programmed cell death pathways, including

autophagy, entotic cell death, ferroptosis, lysosome-dependent cell death, necroptosis, and pyroptosis, which returned to their normal levels after dietary reversal (Supplementary Fig. 1A).

In summary, the phenotypic and transcriptional data collectively demonstrate the beneficial effects of an 8-week dietary reversal on MASLD-related pathologies.

Certain transcriptional changes persist within the liver even after dietary transition

Although the primary features of MASLD were successfully resolved post-dietary reversal, some specific detrimental molecular events induced by the WD in the liver have not been completely eliminated, as suggested by clear separation in the PCA plot between WD and WD→CD groups (Fig. 2A). We next compared gene expression among the three groups to discover the differential genes resistant to reversal by dietary intervention. This analysis identified 58 consistently upregulated genes in both the WD and WD→CD groups, alongside 53 consistently downregulated genes in these groups, compared to the CD group (Fig. 3A-B). Among these 111 consistently differential genes, 50 upregulated (Geneset 1) and 40 downregulated (Geneset 2) genes aligned with human homologs, with the remainder being unique to the mouse genome. Detailed expression patterns and intergroup statistical metrics of these homologous genes are outlined in Figures 3C-D and Supplementary Tables 7–10, respectively.

To better understand the persistent alterations in specific biological processes and molecular functions during dietary transition, Gene Ontology pathway enrichment analysis was conducted on both Geneset 1 and Geneset 2. Notably, the Gene Ontology biological processes function annotations demonstrated consistent upregulation of pathways related to lipid localization, leukocyte cell-cell adhesion, and lipid transport (Fig. 3E). Conversely, pathways associated with steroid metabolic process, sterol metabolic process, and carboxylic acid catabolic process remained downregulated despite the dietary shift (Fig. 3F). Moreover, the Gene Ontology molecular function annotations shed light on the molecular activities influenced by the consistently dysregulated genes. Post dietary reversal, pathways linked to receptor-ligand activity, signaling receptor activator activity, and growth factor activity (Supplementary Fig. 1B) continued to exhibit heightened activation, while the molecular functions involving organic acid binding, oxidoreductase activity, and retinoic acid 4-hydroxylase activity sustained repression (Supplementary Fig. 1C). These findings suggest that despite the successful histological resolution of steatosis, the persistence of dysregulated genes associated with lipid and steroid metabolism pathways indicates that certain molecular imprints induced by the WD persist even after dietary intervention.

DDR pathway activation and P53 accumulation are ongoing in mice liver after switching back from WD to CD

Although we identified consistently regulated genes and their enriched pathways in both WD and WD→CD groups, the specific WD-induced signaling pathways that remain active and exert a prominent influence on the liver after transitioning from WD to CD are still unknown. To decipher these ongoing WD-mediated pathways persisting in the liver even after transitioning from a WD to a CD, GSEA analysis with reference to the WikiPathways database identified 195 significantly upregulated pathways in the WD group and 14 pathways in the WD→CD group compared to the CD group. The subsequent overlap between these two pathway sets revealed only
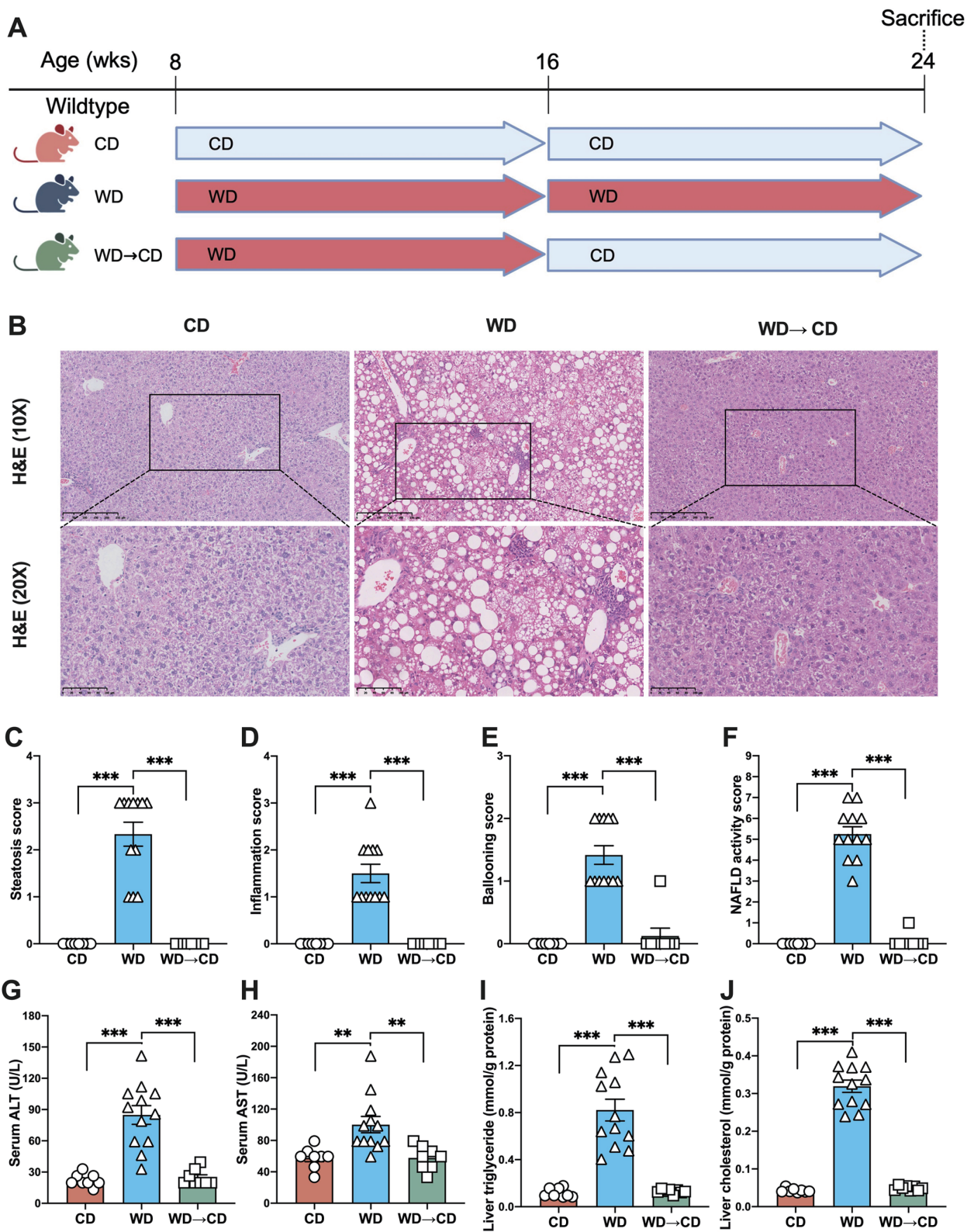
Fig. 1. Dietary reversal from the Western diet (WD) back to the chow diet (CD) successfully ameliorated liver injury and lipid metabolism in mice fed a WD. (A) Study design, (B) representative images of liver sections stained with hematoxylin and eosin, (C-F) nonalcoholic fatty liver disease activity score, (G) serum alanine aminotransferase, (H) serum aspartate aminotransferase, (I) liver triglyceride, and (J) liver cholesterol are shown. n = 8–12 per group. Data are presented as Mean ± SEM. **$p < 0.01$; ***$p < 0.001$. H&E, hematoxylin and eosin.
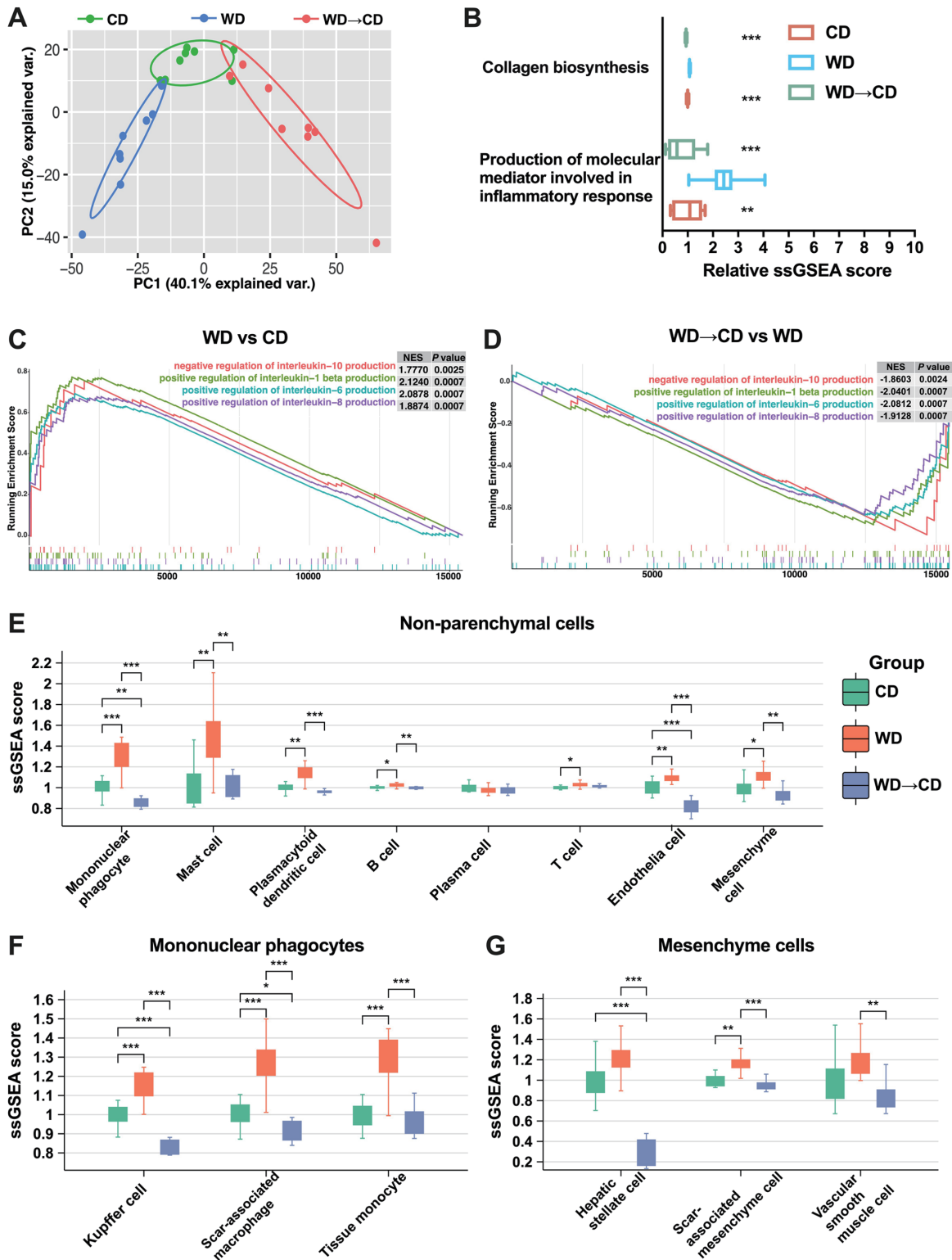
Fig. 2. Dietary reversal normalized the enrichment level of genes and pathways related to inflammation and fibrosis in the liver. (A) Principal component analysis plot displaying transcriptomic expression patterns in the murine liver of three groups. (B) The deconvolution scores of pathways in the murine liver of three groups. All values were compared to the WD group. (C-D) Gene set enrichment analysis exhibited that pathways of cytokine production were significantly activated in the 16-week WD group compared to the 16-week CD group and dramatically suppressed after an 8-week dietary reversal. The enrichment levels of overall non-parenchymal cells (E), mononuclear phagocytes (F), and mesenchyme cells (G) in three groups. n = 8 per group. Data are centered and presented as Mean ± SEM. *p < 0.05; **p < 0.01; ***p < 0.001. WD, western diet; CD, chow diet; ssGSEA, Single-sample Gene Set Enrichment Analysis.
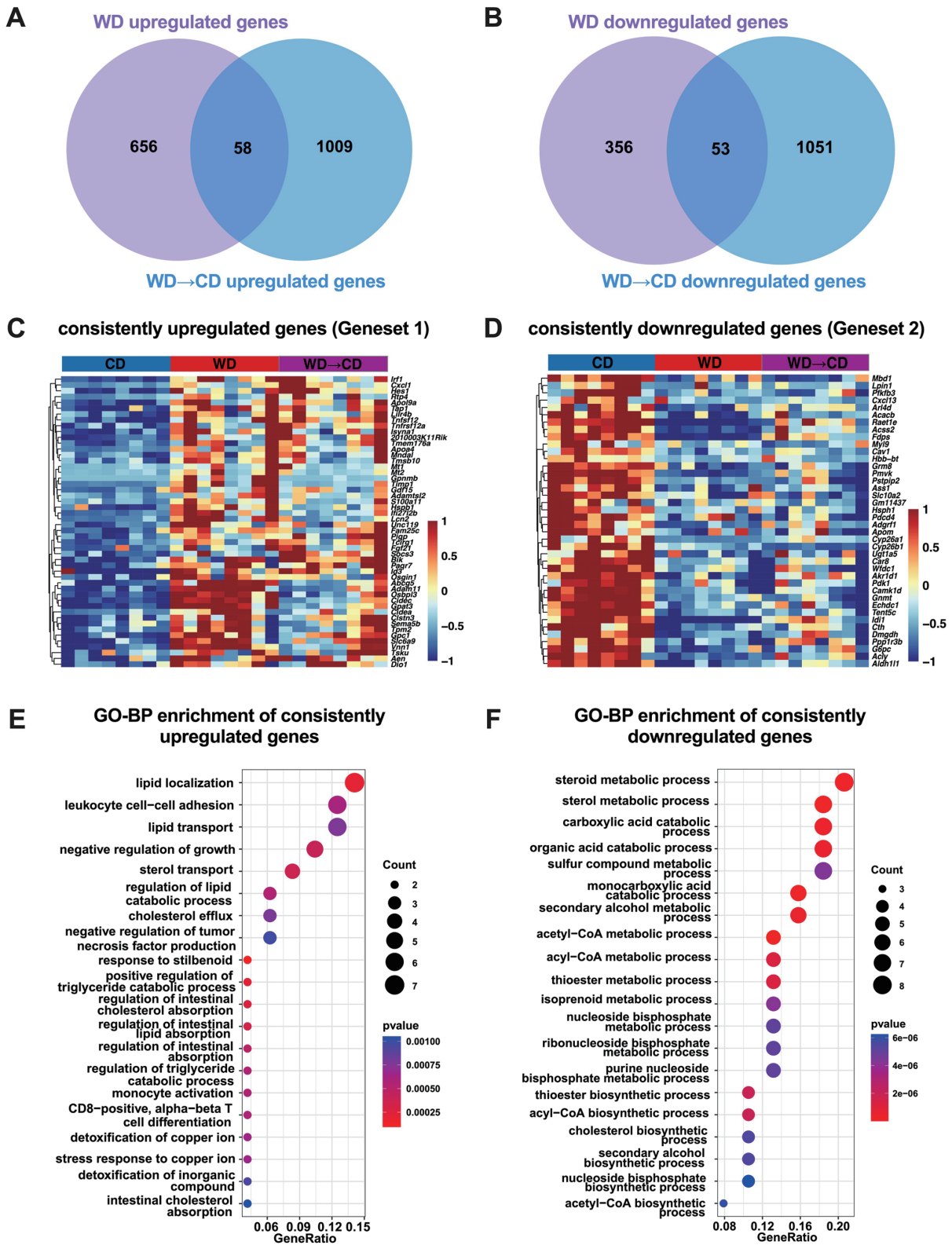
Fig. 3. Persistent liver transcriptional alterations observed in mice after switching back from WD to CD. (A-B) Venn diagram showing 58 consistently upregulated genes and 53 consistently downregulated genes in both the 16-week WD group and the WD→CD group. (C-D) The expression patterns of 58 consistently upregulated genes and 53 consistently downregulated genes in three groups. n = 8 per group. (E-F) Gene Ontology biological processes enrichment analysis of consistently upregulated genes and consistently downregulated genes, respectively. WD, western diet; CD, chow diet; GO-BP, Gene Ontology-Biological Process.

the DDR and miRNA regulation of DDR pathways as significantly upregulated in both the WD and WD→CD groups (Fig. 4A). Additionally, ssGSEA analysis showed a 1.5-fold enrichment of the DDR pathway in both groups compared with the CD group (Fig. 4B).

To understand the potential association between the persistent effects of WD and the activation of the liver DDR pathway, genes increased in the DDR pathway in both the WD and WD→CD groups were investigated. Seven genes were identified: *Bax*, *Gadd45a*, *Cdk4*, *Trp53*, *Mdm2*, *Rad1*, and *Ccnd3* (Supplementary Fig. 2A-B). Notably, *Trp53*, encoding for the transcriptional factor P53, exhibited the highest NAFLD relevance score among these genes, indicating its potential implication in MASLD progression (Fig. 4C). In mouse liver, the transcriptional levels of *Trp53* were relatively higher in both the WD and WD→CD groups compared to the CD group (Fig. 4D). Moreover, western blot analysis demonstrated elevated expression levels of P53 and phospho-histone H2A.X (γ-H2A.X), a DDR marker, in both the WD and WD→CD groups (Fig. 4E, F). Furthermore, ssGSEA analysis indicated higher expression of P53 target genes in both groups, compared with the CD group (Supplementary Fig. 2C-D). These findings demonstrated the consistent activation of the DDR pathway and the elevated expression of P53 in the liver during WD feeding and post-dietary reversal.

Additional RNA sequencing data from human liver samples (GSE89632) provided insightful observations regarding P53 levels in MASLD patients. Elevation in *TP53* (*TP53* in humans and *Trp53* in mice) levels was notably linked to lobular inflammation and hepatocyte ballooning in MASLD patients. Moreover, a tendency towards a positive correlation between *TP53* levels and liver fibrosis was observed, although statistical significance was not achieved with a *p*-value of 0.09 (Fig. 4G). These findings highlight the potential role of P53 in MASLD pathogenesis, particularly in contributing to hepatic changes associated with inflammation, ballooning, and fibrosis.

History of lipotoxic damage triggers persistent DDR pathway activation in hepatocytes

Persistent activation of the DDR pathway was noted in liver tissue even after the diet reversal, yet it remained unclear if such sustained activation occurred explicitly in hepatocytes. As is widely recognized, PA can instigate lipotoxic damage in hepatocytes, subsequently leading to the activation of the DDR pathway.[44] Therefore, we intervened with Huh7 cells using 0.4 mM PA and incorporated a 24-h PA-free period at different time points in the *in vitro* experiments to simulate the transition from a Western diet to a chow diet in mice, as depicted in Fig. 5A. Starting with a 24-h PA stimulation experiment, we conclusively demonstrated that a 24-h exposure to 0.4 mM PA sufficiently elevates the DDR marker γ-H2A.X, causing the death of over half of the Huh7 cells (Supplementary Fig. 2E-G). Nonetheless, a 24-h PA-free period was insufficient to restore DDR signaling to a normal state, demonstrated by the fact that the PA-PBS group presented higher levels of γ-H2A.X compared to the PBS-PBS group, despite the levels in the former being lower than in the PBS-PA group, which was not withdrawn from PA in the last 24 h (Fig. 5B-C). To ascertain whether prior lipotoxic damage exacerbates the harm upon re-exposure to PA stimulation, we conducted an additional, third round of PA stimulation experiments. The results displayed elevated γ-H2A.X levels and a significant increase in cell death in the PA-PBS-PA group compared to the PBS-PBS-PA group (Fig. 5D-F). This provides a preliminary illustration that a prior history of lipotoxic damage amplifies DNA damage in hepatocytes dur-

ing a secondary hit.

In brief, a history of lipotoxic damage elicits persistent DDR signaling activation in hepatocytes. The effect and detailed mechanism of continuous DDR signaling activation on MASH require further investigation, which will be explored in the following sections.

The positive regulatory role of P53 in the apoptotic signaling pathway in vivo.

The livers of WD→CD mice exhibit elevated P53 expression, a transcriptomic signature compared to CD mice. This elevation in P53 expression aligns with hepatocyte ballooning degeneration, indicative of apoptosis activation.[45] To verify the association between *TP53* and hepatocyte apoptosis in humans, we performed a Spearman correlation analysis on the publicly available RNA sequencing dataset (GEO dataset ID: GSE135251). A notable positive correlation was observed between the expression levels of *TP53* and various apoptosis-related genes, such as *BAX*, *BCL2*, *MYC,* and *TNFRSF10B* (Supplementary Fig. 3A).

To further explore these relationships *in vivo*, the mouse dataset (GEO dataset ID: GSE176112) was utilized, and the gene expression profiles between the livers from P53-null mice and wild-type mice under HFD feeding conditions were compared. Results indicated downregulation of the pathway involved in apoptosis progress in P53-null mice compared to wild-type mice (Supplementary Fig. 3B), suggesting that P53 potentially mediates the apoptosis process in the liver of diet-induced MASLD mouse models. Then, the potential association between apoptotic signaling, lobular inflammation, hepatocellular ballooning, and fibrosis was investigated. ssGSEA analysis revealed a significant parallel correlation between the enrichment level of the extrinsic apoptotic signaling pathway and the scores of liver inflammation, ballooning, and fibrosis, as well as *TP53* expression (Supplementary Fig. 3C).

To conclude, the *in vivo* evidence suggests the potentially harmful effect of P53 in the diet reversal group. These findings accentuate the intricate connections between P53-mediated pathways, liver pathology, and apoptosis in the context of MASLD.

P53 might transcriptionally upregulate Aen to enhance apoptotic signaling in liver

Although the liver in mice that transitioned from WD to CD maintained elevated P53 expression, continuing to activate apoptotic signaling, it remains uncertain whether P53, the primary transcription factor in the DDR pathway, activates the apoptosis process by directly enhancing the transcription of specific genes, especially after discontinuing exposure to WD. To uncover the underlying mechanism, an intersection analysis was conducted between 587 genes downregulated in P53-null mice and the 50 consistently upregulated genes (Geneset 1) in both the WD and WD→CD groups. This analysis identified a sole gene, *Aen*, exhibiting continuously elevated expression in the liver of mice transitioning from WD to CD (Fig. 6A, B). Significant co-expression patterns were observed between *Trp53* and *Aen* in the mouse liver (Supplementary Fig. 4A). Conversely, the knockout of P53 resulted in decreased *Aen* expression by 45% in the liver (Fig. 6C), suggesting the important role of P53 as a positive regulator of *Aen* expression. In human liver, a significant positive correlation was noted between the DDR pathway, *TP53*, and *AEN* (Fig. 6D, E).

Subsequent correlation analyses on human RNA-seq data revealed a notable elevation in *AEN* expression correlated with the NAFLD activity score and fibrosis stage (Fig. 6F,
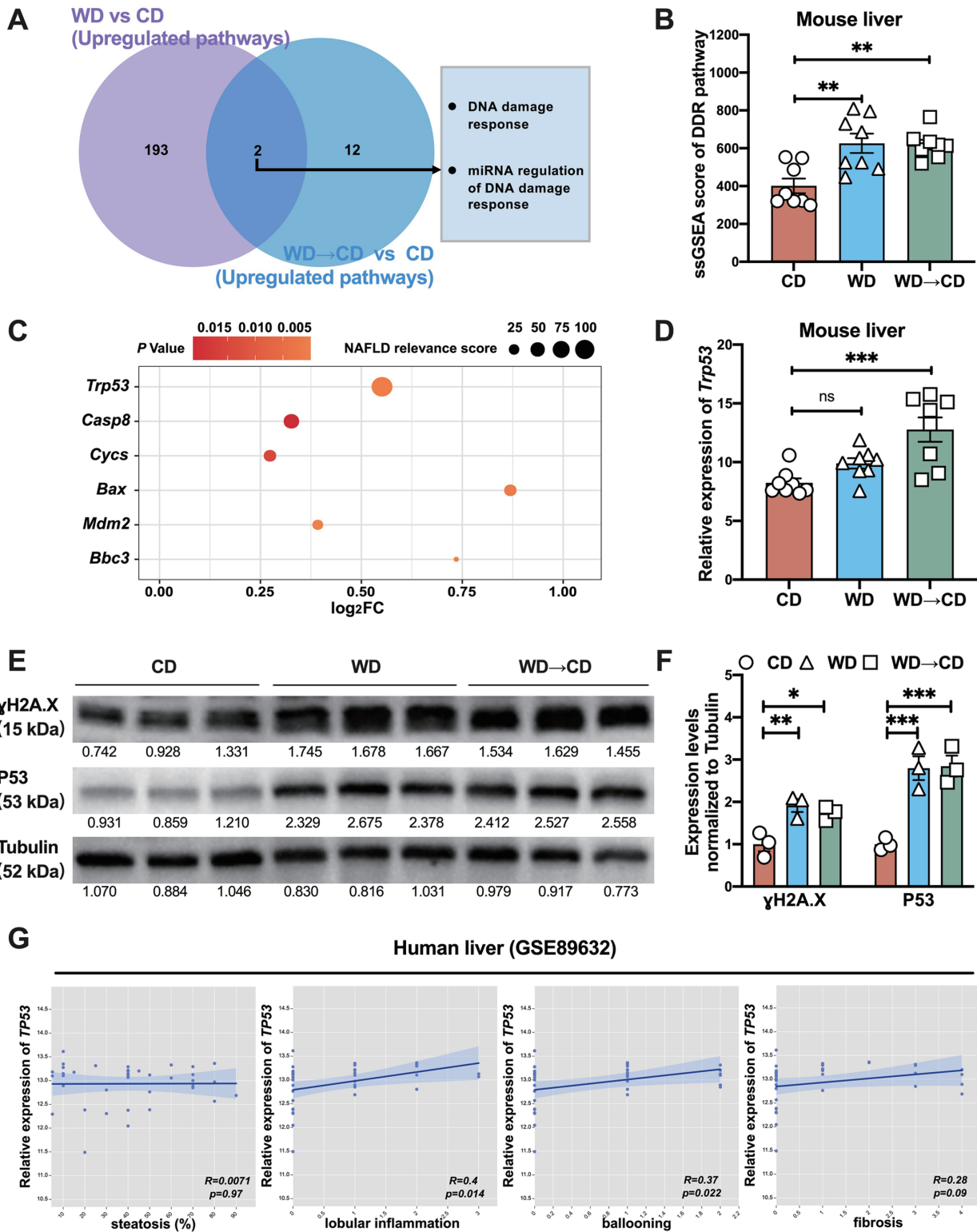
Fig. 4. DNA damage response (DDR) pathway activation and P53 accumulation are ongoing in the murine liver after switching back from WD to CD.
(A) Venn diagram of enriched pathways. (B) The deconvolution scores of DDR. (C) The nonalcoholic fatty liver disease relevance scores for genes increased in both the WD and WD→CD groups in the DDR pathway. (D) Relative mRNA expression of *Trp53* in mice liver. n = 8 per group. Data are presented as Mean ± SEM. (E-F) Protein expression of P53 and phospho-histone H2A.X (γ-H2A.X). n = 3 per group. Data are centered and presented as Mean ± SEM. *$p < 0.05$; **$p < 0.01$; ***$p < 0.001$. (G) Correlation between the mRNA expression level of *TP53* and the histopathological features of metabolic dysfunction-associated steatotic liver disease (MASLD). WD, western diet; CD, chow diet; ssGSEA, Single-sample Gene Set Enrichment Analysis; DDR, DNA damage response.
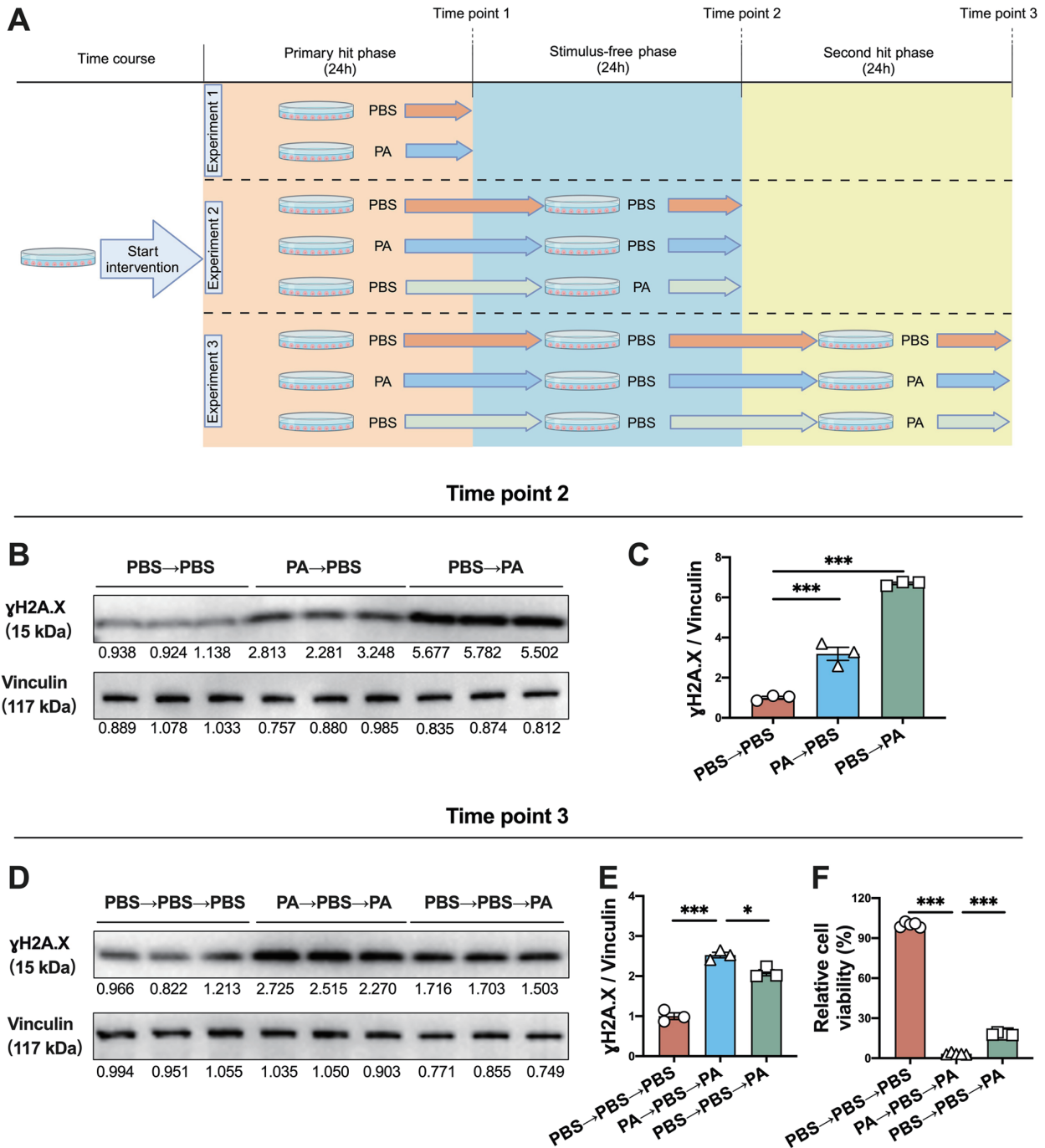
Fig. 5. History of lipotoxic damage triggers persistent DDR pathway activation in hepatocytes. (A) Flow diagram illustrating the three rounds of palmitic acid (PA) stimulation experiments. (B-C) Protein expression of γ-H2A.X at the second designated time point. n = 3 per group. (D-E) Protein expression of γ-H2A.X at the third designated time point. n = 3 per group. (F) Cell viability shown by CCK-8 assays. Data are centered and presented as Mean ± SEM. *$p < 0.05$; ***$p < 0.001$. PBS, phosphate-buffered saline.

G). This implies that *AEN*, as a direct target gene of P53, potentially contributes to MASLD progression. To comprehensively understand the pathological implications of AEN in MASLD, an intersection analysis between genes upregulated in the WD→CD group and genes positively correlated with *AEN* (GEO dataset ID: GSE135251) was conducted. This identified a total of 260 potential downstream genes of AEN

(Fig. 6H). Gene function annotations revealed a considerable positive association between *Aen* expression and the enrichment of the execution phase of apoptosis in the mouse liver (Fig. 6I, J). It is noteworthy that, similar to P53 and AEN, higher enrichment of the execution phase of apoptosis was observed in both WD and WD→CD groups compared to the CD group (Supplementary Fig. 4B). Likewise, in the human
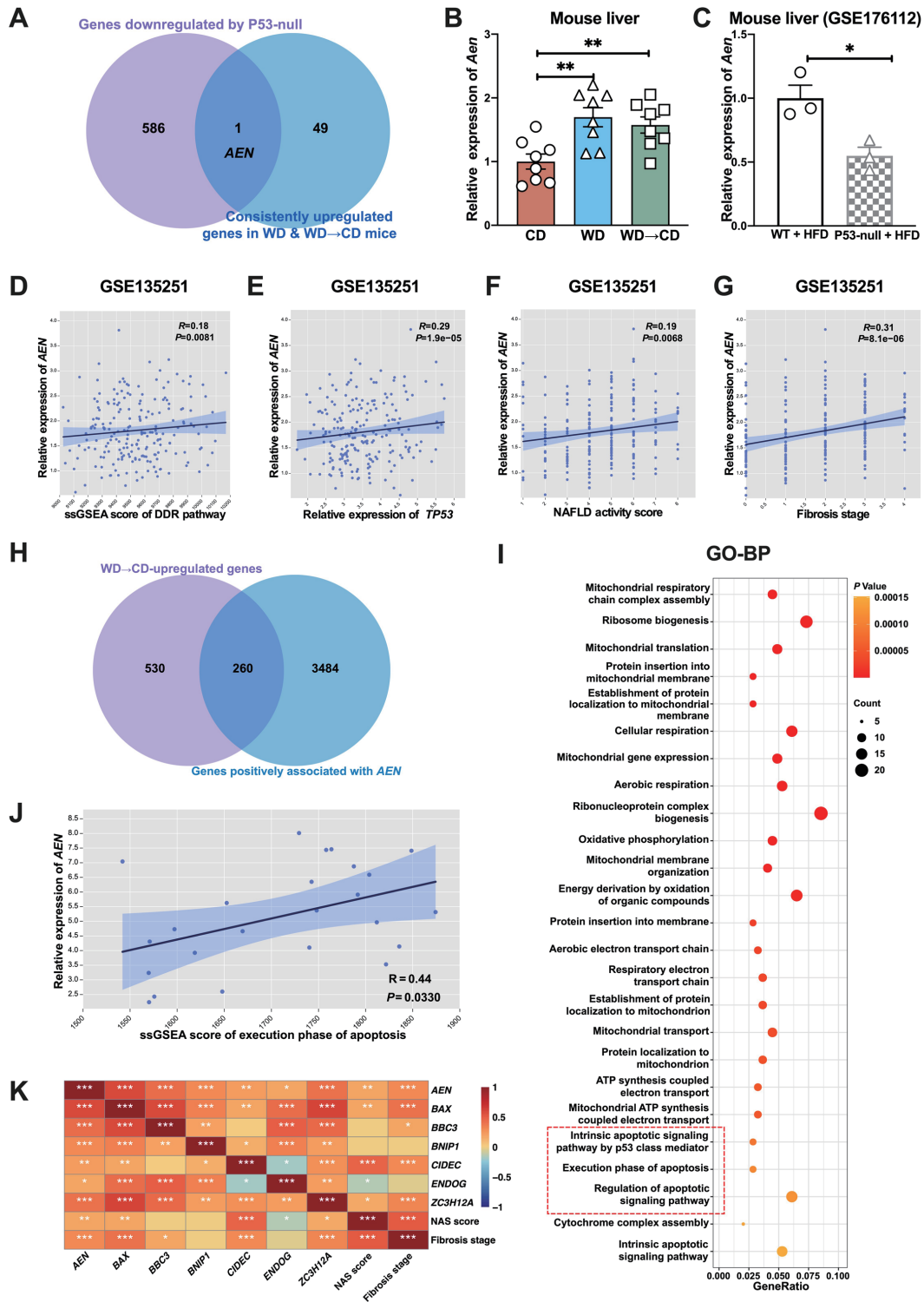
Fig. 6. P53 may upregulate apoptosis-enhancing nuclease (AEN) to enhance apoptotic signaling in the liver after switching back from WD to CD. (A) Venn diagram of gene sets. (B-C) Relative mRNA expression of *Aen* in murine liver. n = 8 per group in Figure 6B. n = 3 per group in Figure 6C. Data are presented as Mean ± SEM. (D-E) Correlation of *AEN* with DDR pathway and *TP53* in human liver. (F-G) Correlation of *AEN* with histopathological features in human liver. (H) Venn diagram displaying the potential downstream gene set of *AEN*. (I) Gene Ontology biological processes enrichment analysis examining the function of the potential downstream gene set of *AEN*. (J) Correlation between *Aen* and the execution phase of apoptosis in mice liver. (K) Correlation between *AEN*, representative genes for the execution phase of apoptosis, and clinicopathological parameters of MASLD in human liver. *$p < 0.05$; **$p < 0.01$. WD, western diet; CD, chow diet; ssGSEA, Single-sample Gene Set Enrichment Analysis; DDR, DNA damage response; HFD, high-fat diets; WT, wild-type; NAFLD, Nonalcoholic fatty liver disease; MASLD, Metabolic dysfunction–associated steatotic liver disease.

liver, a significant co-expression pattern was also observed between *AEN* and representative genes from the pathway of the execution phase of apoptosis (Fig. 6K). These findings suggest a conserved positive regulatory relationship between AEN and the execution phase of apoptosis across mice and humans. Furthermore, as potential downstream signals of AEN, the majority of representative genes in the execution phase of apoptosis were also positively correlated with clinicopathological parameters of MASLD, similar to *AEN* and *Trp53* (Fig. 6K).

In summary, even after transitioning from WD to CD, the liver continues to exhibit persistent upregulation of P53 and its target gene *AEN*. AEN potentially plays a detrimental role in MASLD-associated pathologies by promoting apoptosis.

Discussion

To date, no pharmacological therapies for MASLD have been approved by the FDA.[1,7,46] Although dietary intervention can reverse histological features of MASLD, past exposure to a WD and a history of MASLD might trigger persistent alterations in liver transcriptomic profiles, which have not been fully understood. In this study, we carried out parallel RNA-sequencing in liver tissue from MASLD patients, as well as wild-type and P53-knockout mice across various animal models. Molecular biology experiments and biochemical analyses were undertaken to validate the conclusions drawn from bioinformatics analysis. Along these lines, we observed that reversal from a WD back to a CD alleviated key MASLD-associated features; however, DDR pathway activation and its key transcription factor P53 accumulation persisted in the liver after this reversal, at both the transcriptional and translational levels. Our analysis of MASLD patients unveiled a robust correlation between P53 signaling and hepatocyte ballooning, hinting at the contributory role of elevated P53 in advancing MASH. Additionally, P53 knockout suppressed *Aen* expression and apoptosis signaling, which like P53, remained continuously elevated in the liver even after diet reversal. Mechanistically, following dietary switching, the persistent elevation of P53 could regulate apoptosis through the overexpression of AEN in the liver (Fig. 7).

Initially, it was challenging to identify the persistent detrimental effects of a WD history on MASLD because key markers of lipid metabolism, inflammation, and fibrosis in the liver were normalized after dietary reversal. A breakthrough was made when we conducted RNA-seq, uncovering 58 consistently upregulated genes (including Aen) and 53 consistently downregulated genes in both the 16-week WD group and the WD→CD group. Furthermore, in separate rigorous research, a two-week dietary reversal period was shown to normalize the liver weight and glucose tolerance in mice.[47] Therefore, our transcriptomic signature exhibited persistence, as evidenced by the sufficiency in the dietary reversal period of eight weeks in our study. These altered genes provide direct evidence that a history of consuming a Western diet has long-term effects on liver transcriptomic profiles. Interestingly, functional annotation analysis of the 58 consistently upregulated genes revealed a significant enrichment of the leukocyte cell-cell adhesion pathway, indicating its continuous activation in the liver after diet reversal. This finding partially elucidates why Th17 cells remained highly recruited in the mouse liver in another experimental study despite switching mice from a high-fat and high-fructose diet to a CD.[12]

Furthermore, our findings demonstrate that diet reversal effectively normalized the majority of MASLD-associated features. Nevertheless, the DDR pathway remained unaffected.

In various chronic liver diseases, DNA damage response serves as a hallmark of disease progression exacerbated by compensatory regeneration.[48,49] Activation of DDR is not uncommon in MASLD research. It had been reported in 2002 that there was a higher occurrence of lipid peroxidation and oxidative DNA damage in the livers of MASLD patients compared to healthy controls.[50] Subsequent findings revealed an increased activation of DDR in correlation with hepatocellular ballooning and liver fibrosis in patients with MASLD.[51] Notwithstanding, our study reported the persistent activation of the DDR pathway even after MASLD remission. However, our studies did not determine the upstream mechanisms of the DDR pathway. In MASLD, the liver experiences elevated replication stress, resulting in defective replication forks and subsequent induction of DDR activation.[52] Therefore, sustained cellular replication stress and nucleotide pool imbalance may contribute to the persistent activation of the DDR pathway in the liver, even after MASLD resolution.

To understand the impact of the DDR pathway on MASH, we conducted an in-depth exploration of the transcriptomic landscape modulated by the primary DDR transcription factor, P53, which is persistently upregulated after dietary switching back to CD. This observation is expected, as P53 functions as a primary stress sensor with regulatory control over diverse biological processes.[53] The persistent cellular proliferation stress during the development and resolution of MASLD may result in increased levels of P53. Additionally, P53 overexpression was primarily observed in hepatocytes during the development of MASLD.[54] Furthermore, we revealed a positive correlation between the transcription levels of P53 and lobular inflammation as well as hepatocyte ballooning, while no correlation was observed with hepatic steatosis. A separate prior study observed a gradual elevation in P53 levels corresponding to the severity of liver fibrosis.[53] However, in our study with a larger sample size of human subjects, the relationship trend between transcription levels of P53 and liver fibrosis did not achieve statistical significance. There is a demand for expanded cohorts comprising large samples of MASLD patients with protein data to investigate the correlation between P53 expression and key pathological characteristics of MASLD.

The involvement of increased P53 in MASLD has been thoroughly investigated. In a prior report, it was found that P53 deficiency alleviated hepatic lipid accumulation, inflammatory cell infiltration, and liver fibrosis in a methionine- and choline-deficient diet-induced MASH mouse model.[53] Moreover, another study showed that the P53 inhibitor, pifithrin-α p-nitro, reduced liver triglyceride accumulation in mice fed an HFD.[55] In our study, we observed higher expression levels of P53 in both the 16-week WD group and the WD→CD group compared to the CD group. However, the MASLD pathological features, including hepatic steatosis, lobular inflammation, hepatocyte ballooning, and liver fibrosis, did not worsen following the P53 increase in the WD→CD group. A possible reason is that despite the increase of hepatic P53 in the WD→CD group, the protein level did not rise to the level observed in the 16-week WD group, and its activity as a transcription factor did not rise to the same level. However, we propose that due to the higher levels of P53 than the baseline level, individuals who have previously had MASLD are more susceptible to developing MASLD again after a second Western diet intervention compared to individuals who have not previously had MASLD.

In the liver of MASLD, the promoting effect of P53 on hepatocyte apoptosis appeared to be evident, while the mechanism of P53-induced apoptosis was highly dynamic and influenced by the conditions and duration of MASLD mod-
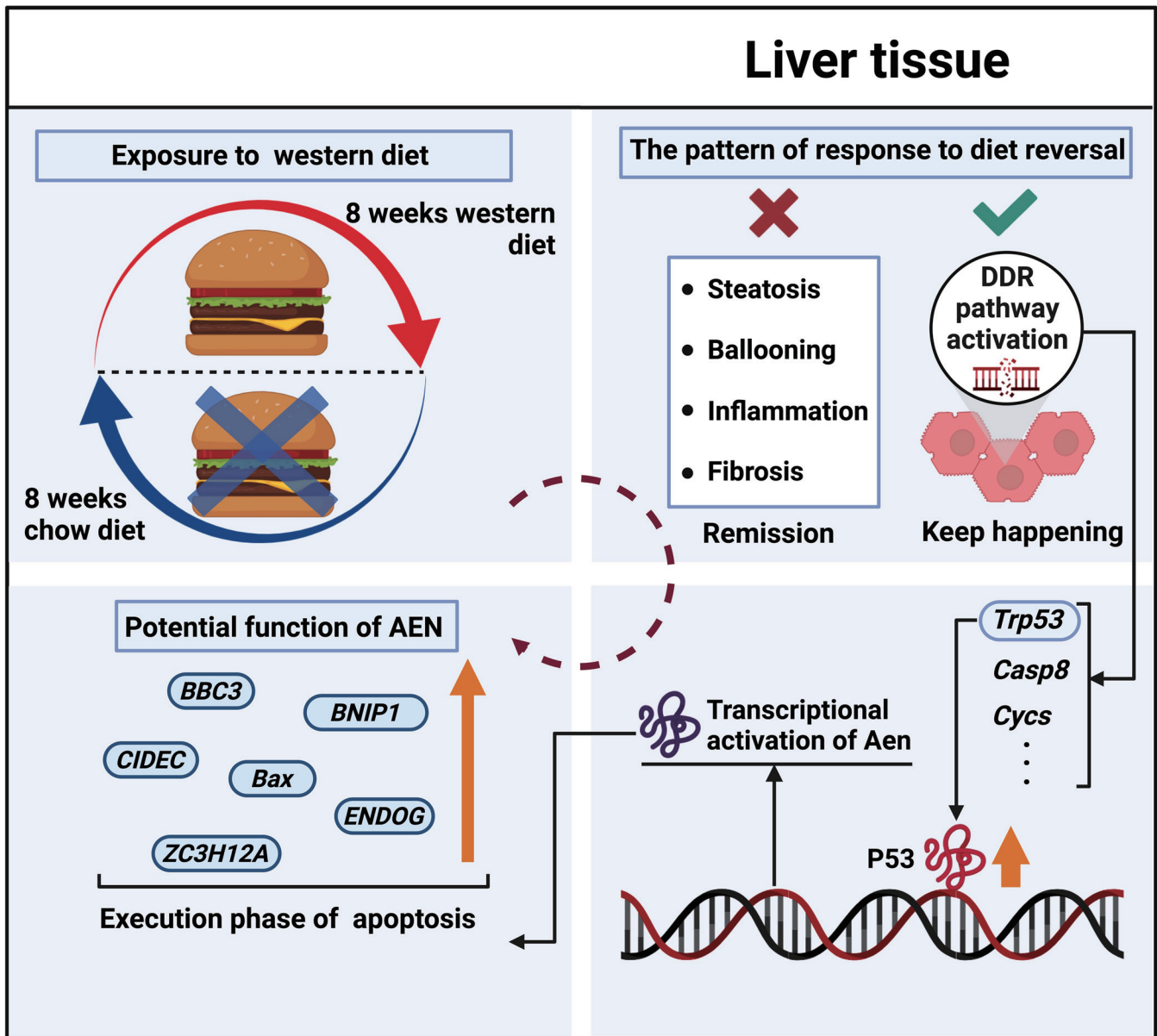
Fig. 7. Proposed model for the persistent activation of DDR signaling and P53-AEN axis in the liver after transitioning from a WD to a CD even when MASLD is histologically resolved. WD, western diet; CD, chow diet; DDR, DNA damage response; AEN, apoptosis-enhancing nuclease; MASLD, Metabolic dysfunction–associated steatotic liver disease.

eling.[53,55,56] It had been reported that in the MASH liver, P53 deficiency reversed the increase of p66Shc signaling, which contributed to the upregulation of cellular reactive oxygen species levels and apoptosis.[53,57] In the present study, we revealed that apoptosis was activated in the mouse liver from both the WD→CD group and the WD group. Additionally, apoptosis was suppressed in the liver of P53 knockout mice. Our findings supported that P53 induces apoptosis in the liver of MASLD and demonstrated that apoptosis signaling remained consistently activated, even after diet reversal. Additionally, through intersection analysis, we inferred that AEN might be another downstream signal of P53, both under or after exposure to WD. AEN is a conventional nucleic acid exonuclease highly efficient at processing 3' DNA ends.[58] It is directly

transcribed by activated P53 and promotes both single- and double-stranded DNA and RNA digestion.[20] Our study demonstrated that P53 knockout inhibited the expression of *Aen* in the liver. Of note, AEN is strongly positively associated with the NAFLD activity score in patients, suggesting a potential pathogenic role of AEN in MASLD. However, there is currently no knowledge about the downstream mechanisms of AEN in MASLD. Further experimental studies are needed to confirm the pro-apoptotic effect of AEN in MASLD. In addition to the DDR/P53/apoptosis axis, two key protective factors associated with obesity, GDF15 and FGF21,[59,60] are persistently upregulated in MASLD. These factors may represent self-protection mechanisms under disease conditions.

Our study has several strengths as well as weaknesses.

Specifically, we identified the hepatic pathological events induced by past exposure to WD, showing not only the persistent activation of DDR signaling and accumulation of P53 post-dietary reversal but also mechanistically establishing the role of P53 in the apoptosis process within MASLD livers. On the other hand, despite our findings demonstrating persistent activation of the DDR pathway, further validation with DDR inhibitors such as Olaparib and Niraparib is required in the MASH mouse model.[61] Of note, the pan-DDR inhibitors, oral vitamin E, and hydroxytyrosol have recently been shown to improve both DNA damage and hepatic steatosis,[62–64] thereby suggesting hepatic DDR signaling as a promising target for both relapse prevention and treatment of MASLD. Secondly, the current study lacks experiments to demonstrate whether individuals who have previously experienced MASLD are more prone to develop MASLD again when compared to those who have never had MASLD before. Further experimental studies on this matter are necessary. Thirdly, apart from the activation of DDR signaling, other pathways such as lipid transport and steroid metabolic processes continue to display aberrant enrichment following dietary reversal. Experimental validation and exploration of the underlying mechanisms will be discussed in our subsequent publication.

Conclusions

The liver concurrently upregulates the DDR signaling and the P53-AEN axis, even after switching back from WD to CD. This suggests that although dietary reversal alleviates key MASH-associated characteristics, several liver signals are not fully normalized and could potentially contribute to MASH progression. More data are required to determine if a history of MASLD could increase DDR signaling enrichment and P53 expression in the human liver, even after MASLD remission. Additionally, the sustained alterations in specific biological processes, including DDR, despite dietary changes suggest a lasting impact of the initial dietary habits on liver molecular signaling. Understanding these persistent molecular events post-dietary reversal is crucial for elucidating the lingering effects of dietary patterns on liver health and metabolism. Further exploration of these pathways may offer insights into potential therapeutic targets or interventions to address the enduring effects of dietary transitions on liver function.

Funding

Conflict of interest

JGF has been an associate editor of the *Journal of Clinical and Translational Hepatology* since 2013. The other authors have no conflicts of interest related to this publication.

Author contributions

Mouse keeping and husbandry (ZYZ, TYR, MYW, LJH), analysis of RNA sequencing data (ZYZ, JQL, SZL), carrying out of experiments and data analysis (ZYZ, JQL, TYJ, YYW, XZG, YYS, RXY), conceptualization and design of the study (CX, JGF), original draft preparation (ZYZ, JQL, TYR, CX, JGF), supervision of the study (CX, JGF). All authors read and approved the final manuscript.

Ethical statement

All animal handling and experimental procedures were approved by the Animal Care and Use Committee of Xinhua Hospital Affiliated to Shanghai Jiao Tong University School of Medicine (Approval No. XHEC-STSCM-2022-163). All animal received human care.

Data sharing statement

The datasets used and analyzed during the current study are available from the corresponding author upon reasonable request.

References

[1] Wong VW, Ekstedt M, Wong GL, Hagström H. Changing epidemiology, global trends and implications for outcomes of NAFLD. J Hepatol 2023;79(3):842–852. doi:10.1016/j.jhep.2023.04.036, PMID:37169151.

[2] Semmler G, Datz C, Trauner M. Eating, diet, and nutrition for the treatment of non-alcoholic fatty liver disease. Clin Mol Hepatol 2023;29(Suppl):S244–S260. doi:10.3350/cmh.2022.0364, PMID:36517001.

[3] Rinella ME, Lazarus JV, Ratziu V, Francque SM, Sanyal AJ, Kanwal F, *et al*. A multisociety Delphi consensus statement on new fatty liver disease nomenclature. J Hepatol 2023;79(6):1542–1556. doi:10.1016/j.jhep.2023.06.003, PMID:37364790.

[4] Simon TG, Roelstraete B, Hagström H, Loomba R, Ludvigsson JF. Progression of non-alcoholic fatty liver disease and long-term outcomes: A nationwide paired liver biopsy cohort study. J Hepatol 2023;79(6):1366–1373. doi:10.1016/j.jhep.2023.08.008, PMID:37604268.

[5] Zeng J, Zhao D, Tai YL, Jiang XX, Su LY, Wang X, *et al*. Dysregulated sphingolipid metabolism contributes to NASH-HCC disease progression. PHYSIOLOGY 2023;38:S1. doi:10.1152/physiol.2023.38.S1.5734514.

[6] Nguyen VH, Ha A, Rouillard NA, Le RH, Fong A, Gudapati S, *et al*. Differential Mortality Outcomes in Real-world Patients with Lean, Nonobese, and Obese Nonalcoholic Fatty Liver Disease. J Clin Transl Hepatol 2023;11(7):1448–1454. doi:10.14218/JCTH.2023.00016, PMID:38161493.

[7] Ryan MC, Itsiopoulos C, Thodis T, Ward G, Trost N, Hofferberth S, *et al*. The Mediterranean diet improves hepatic steatosis and insulin sensitivity in individuals with non-alcoholic fatty liver disease. J Hepatol 2013;59(1):138–143. doi:10.1016/j.jhep.2013.02.012, PMID:23485520.

[8] Sripongpun P, Churuangsuk C, Bunchorntavakul C. Current Evidence Concerning Effects of Ketogenic Diet and Intermittent Fasting in Patients with Nonalcoholic Fatty Liver. J Clin Transl Hepatol 2022;10(4):730–739. doi:10.14218/JCTH.2021.00494, PMID:36062288.

[9] Ma J, Hennein R, Liu C, Long MT, Hoffmann U, Jacques PF, *et al*. Improved Diet Quality Associates With Reduction in Liver Fat, Particularly in Individuals With High Genetic Risk Scores for Nonalcoholic Fatty Liver Disease. Gastroenterology 2018;155(1):107–117. doi:10.1053/j.gastro.2018.03.038, PMID:29604292.

[10] European Association for the Study of the Liver (EASL)., European Association for the Study of Diabetes (EASD)., European Association for the Study of Obesity (EASO). EASL-EASD-EASO Clinical Practice Guidelines for the management of non-alcoholic fatty liver disease. J Hepatol 2016;64(6):1388–1402. doi:10.1016/j.jhep.2015.11.004, PMID:27062661.

[11] Eslam M, Sarin SK, Wong VW, Fan JG, Kawaguchi T, Ahn SH, *et al*. The Asian Pacific Association for the Study of the Liver clinical practice guidelines for the diagnosis and management of metabolic associated fatty liver disease. Hepatol Int 2020;14(6):889–919. doi:10.1007/s12072-020-10094-2, PMID:33006093.

[12] Van Herck MA, Vonghia L, Kwanten WJ, Julé Y, Vanwolleghem T, Ebo DG, *et al*. Diet Reversal and Immune Modulation Show Key Role for Liver and Adipose Tissue T Cells in Murine Nonalcoholic Steatohepatitis. Cell Mol Gastroenterol Hepatol 2020;10(3):467–490. doi:10.1016/j.jcmgh.2020.04.010, PMID:32360637.

[13] Nakanishi N, Hashimoto Y, Okamura T, Ohbora A, Kojima T, Hamaguchi M, *et al*. A weight regain of 1.5 kg or more and lack of exercise are associated with nonalcoholic fatty liver disease recurrence in men. Sci Rep 2021;11(1):19992. doi:10.1038/s41598-021-99036-y, PMID:34620897.

[14] Younossi ZM, Blissett D, Blissett R, Henry L, Stepanova M, Younossi Y, *et al*. The economic and clinical burden of nonalcoholic fatty liver disease in the United States and Europe. Hepatology 2016;64(5):1577–1586. doi:10.1002/hep.28785, PMID:27543837.

[15] Yip TC, Fan JG, Wong VW. China's Fatty Liver Crisis: A Looming Public Health Emergency. Gastroenterology 2023;165(4):825–827. doi:10.1053/j.gastro.2023.06.008, PMID:37343791.

[16] Polyzos SA, Vachliotis ID, Mantzoros CS. Sarcopenia, sarcopenic obesity and nonalcoholic fatty liver disease. Metabolism 2023;147:155676. doi:10.1016/j.metabol.2023.155676, PMID:37544590.

[17] Hata M, Andriessen EMMA, Hata M, Diaz-Marin R, Fournier F, Crespo-Garcia S, *et al*. Past history of obesity triggers persistent epigenetic

changes in innate immunity and exacerbates neuroinflammation. Science 2023;379(6627):45–62. doi:10.1126/science.abj8894, PMID:36603072.

[18] Archambeaud I, Auble H, Nahon P, Planche L, Fallot G, Faroux R, *et al*. Risk factors for hepatocellular carcinoma in Caucasian patients with non-viral cirrhosis: the importance of prior obesity. Liver Int 2015;35(7):1872–1876. doi:10.1111/liv.12767, PMID:25522809.

[19] Zou S, Zhang C, Xu H, Liu Z, Hu Y, Wang W, *et al*. ISG20L1 acts as a co-activator of DAPK1 in the activation of the p53-dependent cell death pathway. J Cell Sci 2023;136(7):jcs260915. doi:10.1242/jcs.260915, PMID:36855954.

[20] Kawase T, Ichikawa H, Ohta T, Nozaki N, Tashiro F, Ohki R, *et al*. p53 target gene AEN is a nuclear exonuclease required for p53-dependent apoptosis. Oncogene 2008;27(27):3797–3810. doi:10.1038/onc.2008.32, PMID:18264133.

[21] Zhao ZH, Wang ZX, Zhou D, Han Y, Ma F, Hu Z, *et al*. Sodium Butyrate Supplementation Inhibits Hepatic Steatosis by Stimulating Liver Kinase B1 and Insulin-Induced Gene. Cell Mol Gastroenterol Hepatol 2021;12(3):857–871. doi:10.1016/j.jcmgh.2021.05.006, PMID:33989817.

[22] Liu XL, Pan Q, Cao HX, Xin FZ, Zhao ZH, Yang RX, *et al*. Lipotoxic Hepatocyte-Derived Exosomal MicroRNA 192-5p Activates Macrophages Through Rictor/Akt/Forkhead Box Transcription Factor O1 Signaling in Nonalcoholic Fatty Liver Disease. Hepatology 2020;72(2):454–469. doi:10.1002/hep.31050, PMID:31782176.

[23] Kleiner DE, Brunt EM, Van Natta M, Behling C, Contos MJ, Cummings OW, *et al*. Design and validation of a histological scoring system for nonalcoholic fatty liver disease. Hepatology 2005;41(6):1313–1321. doi:10.1002/hep.20701, PMID:15915461.

[24] Wang MY, Wang ZX, Huang LJ, Yang RX, Zou ZY, Ge WS, *et al*. Premorbid Steatohepatitis Increases the Seriousness of Dextran Sulfate Sodium-induced Ulcerative Colitis in Mice. J Clin Transl Hepatol 2022;10(5):847–859. doi:10.14218/JCTH.2021.00315, PMID:36304494.

[25] Pertea M, Pertea GM, Antonescu CM, Chang TC, Mendell JT, Salzberg SL. StringTie enables improved reconstruction of a transcriptome from RNA-seq reads. Nat Biotechnol 2015;33(3):290–295. doi:10.1038/nbt.3122, PMID:25690850.

[26] Florea L, Song L, Salzberg SL. Thousands of exon skipping events differentiate among splicing patterns in sixteen human tissues. F1000Res 2013;2:188. doi:10.12688/f1000research.2-188.v2, PMID:24555089.

[27] Ritchie ME, Phipson B, Wu D, Hu Y, Law CW, Shi W, *et al*. limma powers differential expression analyses for RNA-sequencing and microarray studies. Nucleic Acids Res 2015;43(7):e47. doi:10.1093/nar/gkv007, PMID:25605792.

[28] Chen Y, Zhang X, Dantas Machado AC, Ding Y, Chen Z, Qin PZ, *et al*. Structure of p53 binding to the BAX response element reveals DNA unwinding and compression to accommodate base-pair insertion. Nucleic Acids Res 2013;41(17):8368–8376. doi:10.1093/nar/gkt584, PMID:23836939.

[29] Salvador JM, Hollander MC, Nguyen AT, Kopp JB, Barisoni L, Moore JK, *et al*. Mice lacking the p53-effector gene Gadd45a develop a lupus-like syndrome. Immunity 2002;16(4):499–508. doi:10.1016/s1074-7613(02)00302-3, PMID:11970874.

[30] Ye J, Liang R, Bai T, Lin Y, Mai R, Wei M, *et al*. RBM38 plays a tumor-suppressor role via stabilizing the p53-mdm2 loop function in hepatocellular carcinoma. J Exp Clin Cancer Res 2018;37(1):212. doi:10.1186/s13046-018-0852-x, PMID:30176896.

[31] Yu G, Wang LG, Han Y, He QY. clusterProfiler: an R package for comparing biological themes among gene clusters. OMICS 2012;16(5):284–287. doi:10.1089/omi.2011.0118, PMID:22455463.

[32] Subramanian A, Tamayo P, Mootha VK, Mukherjee S, Ebert BL, Gillette MA, *et al*. Gene set enrichment analysis: a knowledge-based approach for interpreting genome-wide expression profiles. Proc Natl Acad Sci U S A 2005;102(43):15545–15550. doi:10.1073/pnas.0506580102, PMID:16199517.

[33] Kelder T, van Iersel MP, Hanspers K, Kutmon M, Conklin BR, Evelo CT, *et al*. WikiPathways: building research communities on biological pathways. Nucleic Acids Res 2012;40(Database issue):D1301–D1307. doi:10.1093/nar/gkr1074, PMID:22096230.

[34] The Gene Ontology Consortium. The Gene Ontology Resource: 20 years and still GOing strong. Nucleic Acids Res 2019;47(D1):D330–D338. doi:10.1093/nar/gky1055, PMID:30395331.

[35] Ramachandran P, Dobie R, Wilson-Kanamori JR, Dora EF, Henderson BEP, Luu NT, *et al*. Resolving the fibrotic niche of human liver cirrhosis at single-cell level. Nature 2019;575(7783):512–518. doi:10.1038/s41586-019-1631-3, PMID:31597160.

[36] Wang S, Wang R, Hu D, Zhang C, Cao P, Huang J. Machine learning reveals diverse cell death patterns in lung adenocarcinoma prognosis and therapy. NPJ Precis Oncol 2024;8(1):49. doi:10.1038/s41698-024-00538-5, PMID:38409471.

[37] Rebhan M, Chalifa-Caspi V, Prilusky J, Lancet D. GeneCards: a novel functional genomics compendium with automated data mining and query reformulation support. Bioinformatics 1998;14(8):656–664. doi:10.1093/bioinformatics/14.8.656, PMID:9789091.

[38] Vu VQ. ggbiplot: A ggplot2 based biplot. R package version 055. 2011. Available from: http://github.com/vqv/ggbiplot.

[39] Kolde R. pheatmap: Pretty Heatmaps. R package version 1.0. 2019. Available from: https://cran.r-project.org/web/packages/pheatmap/index.html.

[40] Lyu F, Han F, Ge C, Mao W, Chen L, Hu H, *et al*. OmicStudio: A composable bioinformatics cloud platform with real-time feedback that can generate high-quality graphs for publication. Imeta 2023;2(1):e85. doi:10.1002/imt2.85, PMID:38868333.

[41] Chen T, Zhang H, Liu Y, Liu YX, Huang L. EVenn: Easy to create repeatable and editable Venn diagrams and Venn networks online. J Genet Genomics 2021;48(9):863–866. doi:10.1016/j.jgg.2021.07.007, PMID:34452851.

[42] Li J, Miao B, Wang S, Dong W, Xu H, Si C, *et al*. Hiplot: a comprehensive and easy-to-use web service for boosting publication-ready biomedical data visualization. Brief Bioinform 2022;23(4):bbac261. doi:10.1093/bib/bbac261, PMID:35788820.

[43] Kassambara A. ggpubr:"ggplot2" based publication ready plots. R package version 0.4.0. 2020. Available from: https://CRAN.R-project.org/package=ggpubr.

[44] Akazawa Y, Nakashima R, Matsuda K, Okamoto K, Hirano R, Kawasaki H, *et al*. Detection of DNA damage response in nonalcoholic fatty liver disease via p53-binding protein 1 nuclear expression. Mod Pathol 2019;32(7):997–1007. doi:10.1038/s41379-019-0218-8, PMID:30809000.

[45] Machado MV, Cortez-Pinto H. Cell death and nonalcoholic steatohepatitis: where is ballooning relevant? Expert Rev Gastroenterol Hepatol 2011;5(2):213–222. doi:10.1586/egh.11.16, PMID:21476916.

[46] Zou ZY, Zeng J, Ren TY, Shi YW, Yang RX, Fan JG. Efficacy of Intragastric Balloons in the Markers of Metabolic Dysfunction-associated Fatty Liver Disease: Results from Meta-analyses. J Clin Transl Hepatol 2021;9(3):353–363. doi:10.14218/JCTH.2020.00183, PMID:34221921.

[47] Vatarescu M, Bechor S, Haim Y, Pecht T, Tarnovscki T, Slutsky N, *et al*. Adipose tissue supports normalization of macrophage and liver lipid handling in obesity reversal. J Endocrinol 2017;233(3):293–305. doi:10.1530/JOE-17-0007, PMID:28360082.

[48] Anstee QM, Reeves HL, Kotsiliti E, Govaere O, Heikenwalder M. From NASH to HCC: current concepts and future challenges. Nat Rev Gastroenterol Hepatol 2019;16(7):411–428. doi:10.1038/s41575-019-0145-7, PMID:31028350.

[49] Boege Y, Malehmir M, Healy ME, Bettermann K, Lorentzen A, Vucur M, *et al*. A Dual Role of Caspase-8 in Triggering and Sensing Proliferation-Associated DNA Damage, a Key Determinant of Liver Cancer Development. Cancer Cell 2017;32(3):342–359.e10. doi:10.1016/j.ccell.2017.08.010, PMID:28898696.

[50] Seki S, Kitada T, Yamada T, Sakaguchi H, Nakatani K, Wakasa K. In situ detection of lipid peroxidation and oxidative DNA damage in non-alcoholic fatty liver diseases. J Hepatol 2002;37(1):56–62. doi:10.1016/s0168-8278(02)00073-9, PMID:12076862.

[51] Nishida N, Yada N, Hagiwara S, Sakurai T, Kitano M, Kudo M. Unique features associated with hepatic oxidative DNA damage and DNA methylation in non-alcoholic fatty liver disease. J Gastroenterol Hepatol 2016;31(9):1646–1653. doi:10.1111/jgh.13318, PMID:26875698.

[52] Donne R, Saroul-Ainama M, Cordier P, Hammoutene A, Kabore C, Stadler M, *et al*. Replication stress triggered by nucleotide pool imbalance drives DNA damage and cGAS-STING pathway activation in NAFLD. Dev Cell 2022;57(14):1728–1741.e6. doi:10.1016/j.devcel.2022.06.003, PMID:35768000.

[53] Tomita K, Teratani T, Suzuki T, Oshikawa T, Yokoyama H, Shimamura K, *et al*. p53/p66Shc-mediated signaling contributes to the progression of non-alcoholic steatohepatitis in humans and mice. J Hepatol 2012;57(4):837–843. doi:10.1016/j.jhep.2012.05.013, PMID:22641095.

[54] Farrell GC, Larter CZ, Hou JY, Zhang RH, Yeh MM, Williams J, *et al*. Apoptosis in experimental NASH is associated with p53 activation and TRAIL receptor expression. J Gastroenterol Hepatol 2009;24(3):443–452. doi:10.1111/j.1440-1746.2009.05785.x, PMID:19226377.

[55] Derdak Z, Villegas KA, Harb R, Wu AM, Sousa A, Wands JR. Inhibition of p53 attenuates steatosis and liver injury in a mouse model of non-alcoholic fatty liver disease. J Hepatol 2013;58(4):785–791. doi:10.1016/j.jhep.2012.11.042, PMID:23211317.

[56] Xu Y, Zhu Y, Hu S, Xu Y, Stroup D, Pan X, *et al*. Hepatocyte Nuclear Factor 4α Prevents the Steatosis-to-NASH Progression by Regulating p53 and Bile Acid Signaling (in mice). Hepatology 2021;73(6):2251–2265. doi:10.1002/hep.31604, PMID:33098092.

[57] Trinei M, Giorgio M, Cicalese A, Barozzi S, Ventura A, Migliaccio E, *et al*. A p53-p66Shc signalling pathway controls intracellular redox status, levels of oxidation-damaged DNA and oxidative stress-induced apoptosis. Oncogene 2002;21(24):3872–3878. doi:10.1038/sj.onc.1205513, PMID:12032825.

[58] Manils J, Marruecos L, Soler C. Exonucleases: Degrading DNA to Deal with Genome Damage, Cell Death, Inflammation and Cancer. Cells 2022;11(14):2157. doi:10.3390/cells11142157, PMID:35883600.

[59] Wang D, Day EA, Townsend LK, Djordjevic D, Jørgensen SB, Steinberg GR. GDF15: emerging biology and therapeutic applications for obesity and cardiometabolic disease. Nat Rev Endocrinol 2021;17(10):592–607. doi:10.1038/s41574-021-00529-7, PMID:34381196.

[60] Tacke F, Puengel T, Loomba R, Friedman SL. An integrated view of anti-inflammatory and antifibrotic targets for the treatment of NASH. J Hepatol 2023;79(2):552–566. doi:10.1016/j.jhep.2023.03.038, PMID:37061196.

[61] Cheng B, Pan W, Xing Y, Xiao Y, Chen J, Xu Z. Recent advances in DDR (DNA damage response) inhibitors for cancer therapy. Eur J Med Chem 2022;230:114109. doi:10.1016/j.ejmech.2022.114109, PMID:35051747.

[62] Mosca A, Crudele A, Smeriglio A, Braghini MR, Panera N, Comparcola D, *et al*. Antioxidant activity of Hydroxytyrosol and Vitamin E reduces systemic inflammation in children with paediatric NAFLD. Dig Liver Dis 2021;53(9):1154–1158. doi:10.1016/j.dld.2020.09.021, PMID:33060043.

[63] Vilar-Gomez E, Vuppalanchi R, Gawrieh S, Ghabril M, Saxena R, Cummings OW, *et al*. Vitamin E Improves Transplant-Free Survival and Hepatic Decompensation Among Patients With Nonalcoholic Steatohepatitis and Advanced Fibrosis. Hepatology 2020;71(2):495–509. doi:10.1002/hep.30368, PMID:30506586.

[64] Scorletti E, Creasy KT, Vujkovic M, Vell M, Zandvakili I, Rader DJ, *et al*. Dietary Vitamin E Intake Is Associated With a Reduced Risk of Developing Digestive Diseases and Nonalcoholic Fatty Liver Disease. Am J Gastroenterol 2022;117(6):927–930. doi:10.14309/ajg.0000000000001726, PMID:35288522.